Influence of Structure of End-group Functionalized Poly(3-hexylthiophene) and Poly(3-octylselenophene) Anchored on Au Nanoparticles

Frederic Monnaie,[†] Lize Verheyen,[†] Julien De Winter,[§] Pascal Gerbaux,[§] Ward Brullot,[‡] Thierry Verbiest,[‡] and Guy Koeckelberghs,[†,]*

[†]Laboratory for Polymer Synthesis, KU Leuven, Celestijnenlaan 200F - box 2404, B-3001 Heverlee, Belgium

‡Laboratory for Molecular Electronics and Photonics, KU Leuven, Celestijnenlaan 200D - box 2425, B-3001 Heverlee, Belgium

[§]Organic Synthesis and Mass Spectrometry Lab, Research Institute for Materials Science and Engineering, University of Mons-UMONS, 23 Place de Parc, B-7000 Mons, Belgium

KEYWORDS Functionalized Ni-initiators, Poly(3-hexylthiophene), conjugated polymers, hybrids, fluorescent quenching

ABSTRACT

Different protected thiol functionalized initiators were prepared and used to polymerize end-functionalized poly(3-hexylthiophene)s in which the spacer between the thiol and the P3HT chain is varied. The protected thiol P3HTs were *in situ* deprotected and anchored onto Au NPs to form P3HT/Au hybrids. The influence of the length of the linker between the P3HT and the Au NP surface on the fluorescence quenching was investigated. The strongest quenching was observed for the shortest linkers. Also a protected thiol poly(3-octylselenophene) (P3OS) was polymerized and anchored together and separately with P3HT to an Au NP. The effect of the presence of P3OS on the quenching was investigated and an additional quenching was observed when P3OS is anchored on the same NP as P3HT. For all polymers ^{1}H NMR and MALDI-ToF analysis confirmed the successful functionalization and the strong control over the polymerization.

INTRODUCTION

When the research groups of McCullough and Yokozawa discovered the controlled chain-growth polymerization of poly(3-hexylthiophene) (P3HT),[1–4] the search to produce materials based on tailor-made conjugated polymers (CPs) began.[5–17] The control over the polymerization allowed researchers to obtain CPs with a defined molecular structure. Besides the advanced structures that can be obtained, a full control over the polymerization also leads to CPs with defined end-groups. If the typical [1,3-bis(diphenylphosphino)propane]dichloronickel (Ni(dppp)Cl_2) initiator is used, the polymer chains are Br/H terminated.[3,18] Different methods can be employed to obtain CPs with specific end-groups. When dealing with a controlled chain-growth polymerization, a

functionalized Grignard reagent can be added to end-cap the polymer chain.[19–22] The Grignard functionality was used to form thiol end-functionalized P3HT chains.[23,24] However, this method is only applicable when dealing with a controlled polymerization. In addition, depending on the Grignard reagent used, both mono- and dicapping can occur, resulting in a contaminated polymer sample. Another approach to introduce a functional end-group is based on post-polymerization reactions. As mentioned before, initiation with $Ni(dppp)Cl_2$ results in a Br/H-terminated polymer and these functionalities can be used to introduce thiol[24], aldehyde[25] or carboxylic acid groups[26]. The use of post-polymerization reactions is rather limited and needs to be performed with very high efficiencies. A more popular approach to introduce functionalized end-groups uses external initiators. This is a more general applicable method, since there is no need for a controlled polymerization mechanism, and a whole variety of functional groups can be introduced at the start of the polymer chain, including various phosphonic esters[27,28], nitroxide[29], (protected) phenol[28], (protected) alcohols[30–32], (protected) acetylene[30,31], (protected) carboxylic acid[30], (protected) amine[30], (protected) thiol[28] and pyridine[28]. It is important to realize that the initiators are synthesized in an independent step. In order to prevent the formation of unfunctionalized polymers, the purity of the initiator is of prime importance when using these external initiators.

One asset of functionalized CPs is the possibility to further prepare block copolymers.[29,30,33,34] Besides the formation of block copolymers, the functional initiators/groups can be used to anchor CPs on different kind of surfaces or substrates or nanoparticles (NPs), hereby making structures with unique properties.[35,36] The properties are not a simple superposition of the properties of the components, but a clear interaction between both components arises. Depending on the targeted inorganic substrate, a specific functional group must be employed.[21,28,37] In the past, thiol-functionalized P3HT in combination with Au NPs have proven to be ideal candidates to form

CP/NP hybrids. This strategy was also used to prepare organic/inorganic hybrid structures in a grafting-from approach.[38–42]

In the present work, we report different protected thiol functionalized P3HT that will be anchored onto Au NPs. Since the properties of a hybrid are not expected to be a superposition of those of the components, but that the components can strongly interact with each other, two parameters will be investigated. First, various initiators are prepared and the effect of the length of the linker on the fluorescence quenching by the Au NP will be investigated. Next, it is investigated whether a quenching of the P3HT fluorescence can also be realized by attachment of a moiety that quenches the P3HT on the same NP, bringing them in close proximity. Therefore, the Au NP will be covered by both P3HT and poly(3-octylselenophene) (P3OS) and the quenching of the P3HT fluorescence by the P3OS will be investigated. All used CPs are presented in Figure 1.

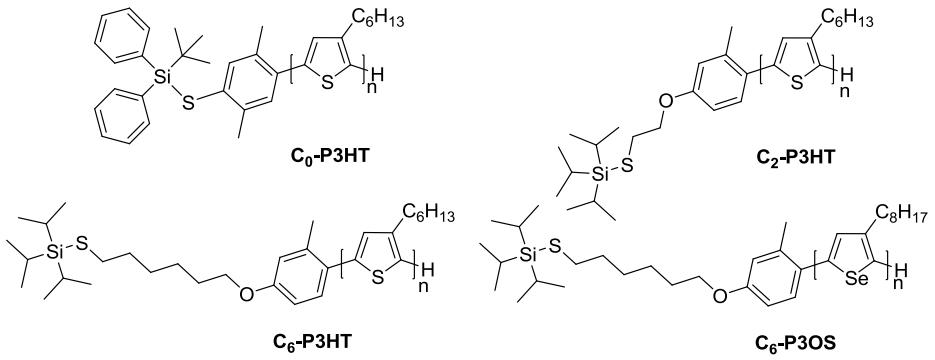

Figure 1. Overview of P3HTs and P3OS end-functionalized polymers.

EXPERIMENTAL SECTION

Reagents and Instrumentation. All reagents were purchased from TCI, Sigma-Aldrich, Acros Organics and ABCR. Reagent grade solvents were dried by a solvent purification system MBRAUN SPS 800 (columns with activated alumina). The gel permeation chromatography (GPC) measurements were performed using a Shimadzu 10A apparatus with a tunable absorbance detector and a differential refractometer in tetrahydrofuran as eluent calibrated toward polystyrene standards. ^{1}H nuclear magnetic resonance (^{1}H NMR) measurements were carried out with a Bruker Avance 300 MHz. ^{31}P NMR measurements were carried out with a Bruker Avance 400 MHz. The mass spectrometric experiments were performed on a large scale tandem mass spectrometer (Waters AutoSpec 6F, Manchester, UK) having an E1B1E2E3B2E4 geometry, where E stands for electrostatic sector and B for magnetic sector. The electron ionization mass spectra (EI-MS) were recorded by scanning the field of the first magnetic sector (B1). The mass-separated ions were counted using an off-axis photomultiplier located after the second electrostatic sector. Typical source conditions were 8 kV accelerating voltage, 200 μA trap current, 200°C source temperature and 70 eV ionizing electron kinetic energy. The solid samples were introduced with a direct insertion probe, whereas the liquid samples were injected into the ion source via a heated septum inlet (160 °C). The accurate mass measurements were recorded using perfluorokerosene (PFK) as the internal calibrant by scanning the accelerating voltage (voltage scan) and increasing the resolution of the mass spectrometer to R = 10.000 at 5% of the peak intensity. UV-vis measurements were performed on a Varian Cary 400 spectrophotometer using a Hellma Quartz Suprasil cell (160.001-QS, path length 10 mm). Emission spectra were recorded on an Edinburgh Instruments FS900 steady-state spectrofluorimeter using a Hellma Quartz Suprasil cell (160.001-QS, path length 10 mm). The spectrofluorimeter is equipped with a 450 W Xenon Arc lamp and extended red-sensitive

photomultiplier (185–1010 nm, Hamamatsu R 2658P), the excitation wavelength was set to 440 nm for all samples. Mass spectra were recorded using an Agilent HP5989. Matrix-assisted laser desorption/ionization time-of-flight (MALDI-ToF) mass spectra were recorded using a Waters QToF Premier mass spectrometer equipped with a Nd-YAG laser of 355 nm with a maximum pulse energy of 65μJ delivered to the sample at 50 Hz repeating rate. Time-of-flight mass analyses were performed in the reflection mode at a resolution of about 10 000. The matrix, trans-2-[3-(4-tert-butyl-phenyl)-2-methyl-2-propenylidene]malononitrile (DCTB), was prepared as a 40 mg/mL solution in chloroform. The matrix solution (1 μL) was applied to a stainless steel target and air-dried. Polymer samples were dissolved in chloroform to obtain 1 mg/mL solutions. Then, 1 μL aliquots of these solutions were applied onto the target area (already bearing the matric crystals) and then air-dried.[43] The polymer **C_2-P3HT**[32]and precursor monomer **14**[44] were synthesized according to literature procedures. Gold nanoparticles were produced using a modified Turkevich citrate reduction method.[45]

RESULTS AND DISCUSSION

Synthesis of the functionalized CPs.

The functionalized Ni-initiators precursors are prepared by an oxidative insertion of $Ni(PPh_3)_4$ in the appropriately functionalized *o*-tolylbromide. The *o*-tolyl group is used to enhance the stability against disproportionation.[31] As indicated, three different thiol functionalized initiators are required, of which two needed to be prepared. Since Grignard reagents are involved in the polymerization reaction, the thiol functionality in each initiators needs to be protected. An overview of all synthetic steps for the functionalized precursor initiators **3** and **10** is presented in Scheme 1, while initiator **5** was already available from previous research[28]. First, the thiophenol

1 is protected using *tert*-butyl(chloro)diphenylsilane (TBDPSCl) in presence of imidazole. Next, $Ni(PPh_3)_4$ is added in an oxidative insertion step to form the protected thiophenol precursor initiator **3**. To increase the length of the linker between the thiol and the CP, precursor **10** is also prepared. First, **7** is deprotonated by K_2CO_3 and 1,6-dibromohexane is added. Then, the thiol functionality is introduced under its protected from using thioltri(*iso*-propyl)silane (STIPS). HSTIPS is first lithiated with *n*-BuLi in order to react with **8**. As a final step, **9** is added to $Ni(PPh_3)_4$ in order to prepare the precursor initiator **10**.

Scheme 1. Synthesis of the precursor initiator.[a]

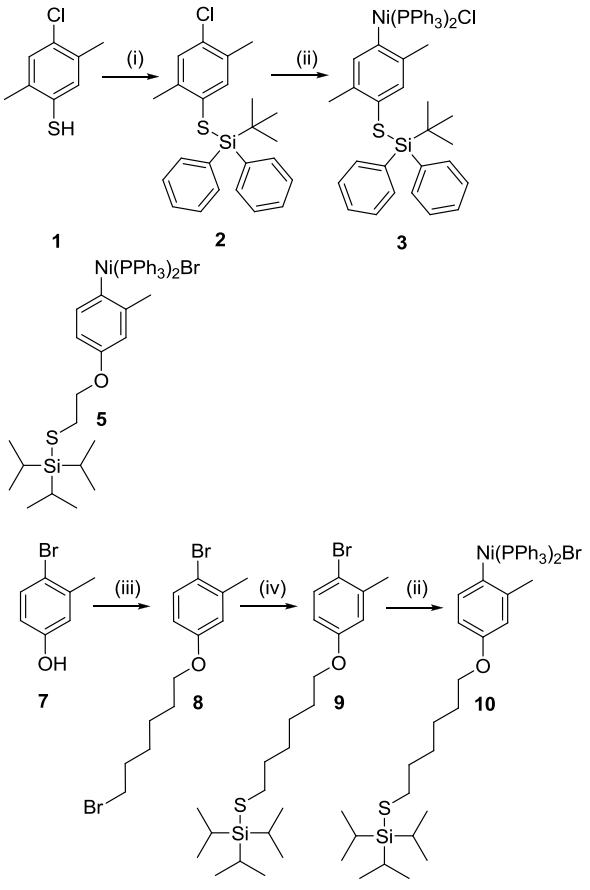

[a]Key: (i) imidazole, TBDPSCl; (ii) $Ni(PPh_3)_4$; (iii) K_2CO_3, 1,6-dibromohexane, KI; (iv) HSTIPS, *n*-BuLi.

All polymers are synthesized based on the Ni(dppp)-mediated Kumada catalyst transfer polycondensation (KCTP) (Scheme 2). For the polymerization of **C_0-P3HT**, **C_2-P3HT** and **C_6-P3HT,** the precursor monomer, 2-bromo-3-hexyl-5-iodothiophene (**12**), is converted to the actual monomer 2-bromo-3-hexyl-5-magnesiochlorothiophene (**13**) using *i*-PrMgCl·LiCl. Prior to initiation, a ligand exchange is performed on the precursor initiator using 2 eq. of 1,3-bis(diphenylphosphino)propane (dppp) in order the generate the actual initiator.[31] Dppp is used as ligand because it, in contrast to PPh_3, leads to a controlled polymerization. This enables us to tune the degree of polymerization (DP) by varying the $[M_0]/[In]$ ratio. This ratio was set to 15 for all polymerizations. This rather low degree of polymerization was chosen in order to allow efficient coupling of the end-groups of the NPs. The polymerization was terminated after 1 h by quenching the mixture with a 2 M HCl solution in THF. The same procedure was used for the synthesis of polymer **C_6-P3OS**, with the sole difference that the GRIM reaction of **14** to **15** was performed at 0 °C to prevent any side reactions.

Scheme 2. Synthesis of polymers **C_0-P3HT**, **C_2-P3HT**, **C_6-P3HT** and **C_6-P3OS**.

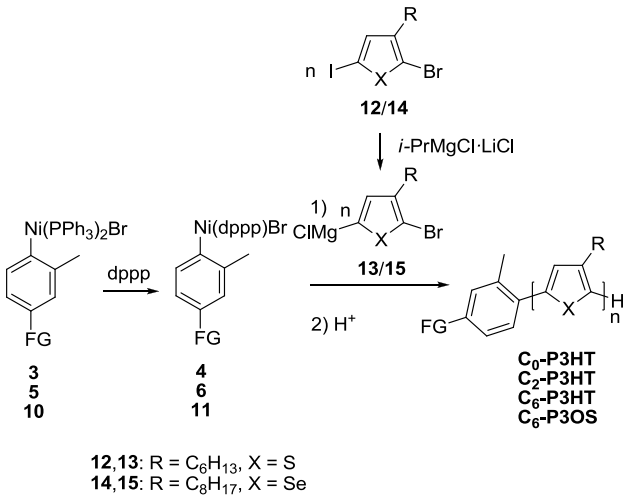

GPC was used to determine the molar mass and dispersity (Đ) of the synthesized polymers **C_0-P3HT**, **C_6-P3HT** and **C_6-P3OS** (Table 1). For all polymers dispersities in the range of 1.1-1.2

were obtained. GPC was calibrated toward polystyrene standards, so care should be taken in the interpretation of the results because molecular masses are overestimated.[46]

Table 1. $\overline{M_n}$, Đ and DP for **C_0-P3HT**, **C_2-P3HT**, **C_6-P3HT** and **C_6-P3OS**.

Polymer	$\overline{M_n}$ (kg/mol)[a]	Đ[a]	DP[b]
C_0-P3HT	3.5	1.2	13
C_2-P3HT	4.1	1.2	16
C_6-P3HT	4.7	1.1	16
C_6-P3OS	4.2	1.1	12

[a] determined by GPC in THF toward polystyrene standard

[b] determined by ^{1}H NMR

When **C_0-P3HT** is analyzed by ^{1}H NMR spectroscopy a whole set of signals is observed - a zoom of the spectrum is presented in Figure 2. The spectrum shows 2 singlets at 2.20 (**a**) and 2.00 ppm (**b**), a multiplet at 2.80 ppm that originates from the internal α-methylene protons (**c**) and more upfield (2.61 ppm) a part of a triplet can be recognized originating from the terminal α-methylene (H-terminated unit) (**d**). No additional triplet around 2.5 ppm (Br-termination) is noticed, which is in line with the controlled nature of the polymerization. Additional signals are observed around 2.43 (**a***) and 2.35 ppm (**b***), possibly originating from the deprotected thiol (due to the addition of HCl to terminate the polymerization). MALDI-ToF confirms the partial deprotection (Figure 2), as well as the fact that all chains are H-terminated and all polymers are successful initiated. This is further confirmed by the fact that **d** ingrates for ~2, while **a**+**a*** and **b**+**b*** integrates for ~3. By combining the information of ^{1}H NMR and MALDI-ToF, the DP is calculated and chain length of 13 units is obtained using Equation 1.

$$DP = \frac{c+d}{\frac{a+b+a*+b*}{6}+\frac{d}{2}} \qquad \text{Equation 1}$$

The ^{1}H NMR spectrum of **C_6-P3HT** (Figure 2) also indicates the presence of the *o*-tolyl function of the initiator function at 2.45 ppm (**a**) and a large peak originating from the internal α-methylene protons (**b,** at 2.80 ppm). The triplet that originates from the terminal α-methylene (**c**) resonates at 2.61 ppm, which indicates that the polymer chains are H-terminated. A second triplet appears at 2.55 ppm and is correlated to the CH_2 group in the linker adjacent to the STIPS functionality. The absence of a clear triplet at 2.57 ppm (Br-terminated terminal α-methylene) demonstrates that polymerization followed a controlled pathway. These findings were also supported by the MALDI-ToF results. The main peaks in the spectrum (Figure 2) correspond to initiator/H-terminated polymer chains. The chain length is calculated based on the integration values of the ^{1}H NMR spectrum and a DP of 16 was derived from this (Equation 2).

The same analysis (Figure 2) was performed on **C_6-P3OS**. The singlet of the *o*-tolyl function of the initiator function appears at 2.44 ppm (**a**), the large peak originating from the internal α-methylene protons (**b,** at 2.73 ppm, somewhat shifted compared to **C_6-P3HT**) and overlapping triplet signals around 2.56 can be observed. MALDI-ToF mass spectrum was measured to identify the actual end-groups of the polymer chains. These measurements reveal that the polymer is initiator/H-terminated, leading to the conclusion that the overlapping signals are a triplet of terminal α-methylene protons of H-terminated thiophene units (**c**) at 2.57 ppm together with a second triplet at 2.55 ppm corresponding to the CH_2 in the linker adjacent to the STIPS functionality. A DP of 12 is calculated using Equation 2.

$$DP = \frac{b+c}{\frac{a}{3}+\frac{c}{2}} \qquad \text{Equation 2}$$

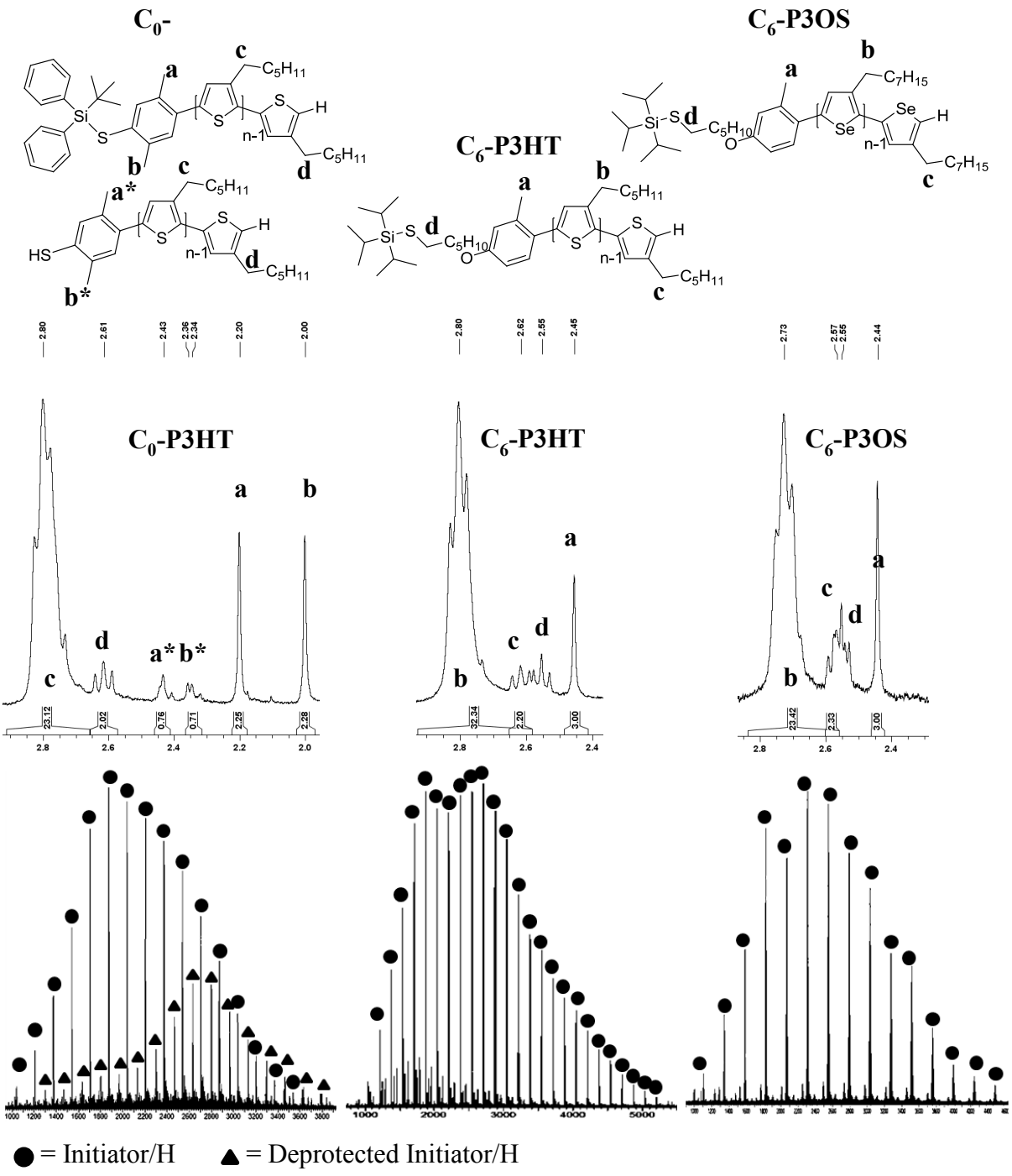

Figure 2. ^{1}H NMR and MALDI-ToF spectra of **C$_0$-P3HT** (left), **C$_6$-P3HT** (middle) and **C$_6$-P3OS** (right).

Synthesis of the hybrids

The formation of the hybrid materials is based on a transfer method in which the functionalized CPs are added to the water soluble citrate-stabilized Au NPs.[47] When applying this transfer method, the strength of the interaction between the functional groups and the NP surface is critical for the success of the displacement of the citrate shell and the anchoring of the functionalized CPs onto the surface. Since deprotection of the functionalized polymer suffers from side-reactions, among which disulfide formation,[28] we tried to unprotect the functional group *in situ*. As already mentioned in the introduction, the effect of the length of the linker on the quenching efficiency will be investigated. So, first 3 different hybrids **C_0-P3HT/Au**, **C_2-P3HT/Au** and **C_6-P3HT/Au** are prepared using respectively **C_0-P3HT**, **C_2-P3HT** and **C_6-P3HT** in combination with the Au NPs. In a second part, the quenching originating from P3OS will also be investigated. Therefore, two additional hybrids are produced. First, the hybrid **C_6-P3HT+C_6-P3OS/Au** is formed by anchoring a 50/50 mixture of **C_6-P3HT** and **C_6-P3OS** on the same Au NP. The final hybrid, namely **C_6-P3OS/Au,** is based on the combination between Au and **C_6-P3OS.** The same procedure is used to synthese all the 5 different hybrids. The CPs are dissolved in $CHCl_3$ and the Au NPs in water, tetraoctylammonium bromide (TOABr) is added as the transfer agent, while tetrabutylammomium fluoride (TBAF) is added to unprotect the thiol-groups. The hybrids are purified using centrifugation and redispersion until a colorless supernatant is observed. Representative TEM images were recorded. They show that the parent Au NPs are clearly present. When the polymer is attached to the NP, the dark Au NP become surrounded by a grey shell, which could tentatively be ascribed to the P3HT. (Figures S20-23)

Influence of the length of the linker on the fluorescence quenching

To verify the fluorescence quenching and the influence of the length of the linker of the anchoring group on the quenching, UV-vis and emission spectroscopy data of **C_6-P3HT**, **C_0-**

P3HT/Au, C_2-P3HT/Au and **C_6-P3HT/Au** are recorded. The distance between the Au NP surface and CP is increased from **C_0-P3HT/Au** to **C_6-P3HT/Au**. In Figure 3 the UV-vis spectra of **C_6-P3HT**, Au, **C_0-P3HT/Au**, **C_2-P3HT/Au** and **C_6-P3HT/Au** are presented. The presence of both the P3HT and the Au nanoparticle is proven by the two transitions in the UV-vis spectrum. Note that it was tried to determine the amount of PH3T in the three hybrids by TXRF, but these measurements failed in determining the amount of S. It is clear that the absorbance of Au is largely influenced by the anchoring of the 2 components. The Au absorbance peaks in the three hybrids is strongly broadened and red-shifted. The red-shift and broadening is more pronounced when a shorter linker is used. This can be explained by the functionalization of the Au surface.[48] The electrons can be delocalized over a larger area, inducing the surface plasmons to resonate at lower energies resulting in a shift of the absorption spectra to longer wavelengths.

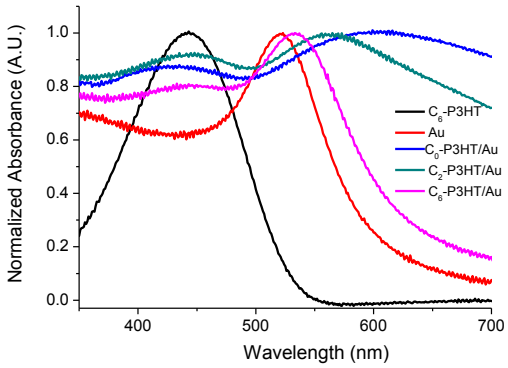

Figure 3. Normalized UV-vis spectra of **C_6-P3HT**, Au, **C_0-P3HT/Au**, **C_2-P3HT/Au** and **C_6-P3HT/Au** in $CHCl_3$.

Upon performing the emission measurements the quenching effect of the Au NPs is investigated for the different hybrids. The Au NP quenches the P3HT by resonant energy transfer from P3HT to the Au NP – a process closely related to Förster energy transfer.[49] The excitation wavelength

is set to 440 nm for all samples. The emission spectra are corrected by the total absorbance at 440 nm (absorbance of the original samples) and also corrected for the absorbance originating from the P3HT present in the hybrids (difference between the hybrid normalized absorbance and the Au normalized absorbance). In this way the difference in Au-amount between the different samples and the background absorbance of Au is accounted for. The fluorescence spectra are presented in Figure 4. Note that the Au NPs do not show any fluorescence upon excitation at 440 nm, so all emission originates from the P3HT present in the hybrids. Compared to **C_6-P3HT** the maximum emission of **C_0-P3HT/Au** is quenched to ~22% of the original emission, to ~30% for **C_2-P3HT/Au** and to ~59% for **C_6-P3HT/Au**. From these results it is clear that the shorter the distance between the CP and the Au NP surface the stronger the quenching. This is in line with a previous study of the influence of the distance between a fluorophore and a (Ag) NP.[50] The fact that the shape of the spectra of the hybrids is the same as that of **C_6-P3HT,** demonstrates that the emission results from isolated P3HT chains. This demonstrates that the P3HT chains anchored to the Au NP do not aggregate; otherwise the shape would resemble that of aggregated P3HT. This is also in line with the UV-vis spectra of the hybrids present in Figure 3. Indeed, aggregation of P3HT results in a strong red-shift. The UV-vis spectra of the hybrids are clearly a superposition of the absorption of Au and isolated but not aggregated P3HT chains. This also confirms that the quenching of the emission is due to the interaction with Au and not to aggregation induced by the anchoring on the Au NPs.

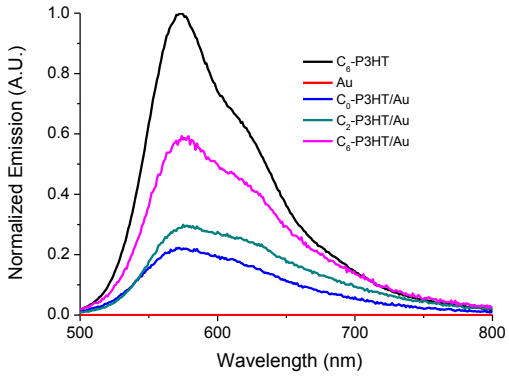

Figure 4. Normalized fluorescence spectra of **C_6-P3HT**, Au, **C_0-P3HT/Au**, **C_2-P3HT/Au** and **C_6-P3HT/Au**; spectra are corrected by the absorption of P3HT at 440 nm.

Influence of the presence on P3OS on the fluorescence quenching

The study above reveals that **C_6-P3HT/Au** hybrids show the strongest fluorescence amongst all the synthesized hybrids. In direct line with this observation, **C_6-P3HT** is combined with **C_6-P3OS** in a 50/50 weight ratio and anchored together on the Au NP surface forming **C_6-P3HT+C_6-P3OS/Au**. UV-vis measurements are performed on the so obtained hybrid **C_6-P3HT+C_6-P3OS/Au** and the results are presented in Figure 5 together with the **C_6-P3HT**, **C_6-P3OS** and Au data. **C_6-P3HT+C_6-P3OS/Au** shows a broad absorption originating from overlapping absorptions of the P3HT, P3OS and Au. This broad peaks confirms the presence of both P3HT and P3OS. Note that although this measurement does not imply that the 1/1 ratio between P3HT and P3OS is respected, this is of no importance: the *presence* of P3OS is investigated, not the influence of its amount.

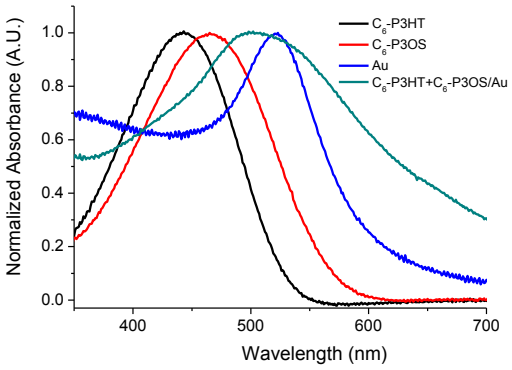

Figure 5. Normalized UV-vis spectra of **C6-P3HT**, **C6-P3OS,** Au and **C6-P3HT+C6-P3OS/Au**; the spectra were measured in $CHCl_3$.

The emission spectra of **C6-P3HT**, **C6-P3HT/Au** and **C6-P3HT+C6-P3OS/Au** are measured to quantify the quenching effect of P3OS (Figure 6). The same absorbance corrections as in the previous experiment are used in order to get a clear view of the quenching effect. When **C6-P3HT** is coupled to the surface of the Au NP in the direct presence of **C6-P3OS**, a clear additional quenching is observed. Compared to **C6-P3HT, C6-P3HT/Au** shows an emission of only ~59% (as was obtained in the previous study), the addition of **C6-P3OS** induces an emission quenching to ~5% of the original **C6-P3HT** signal. This type of quenching was previously observed in block copolymers consisting of P3HT and P3OS.[44]

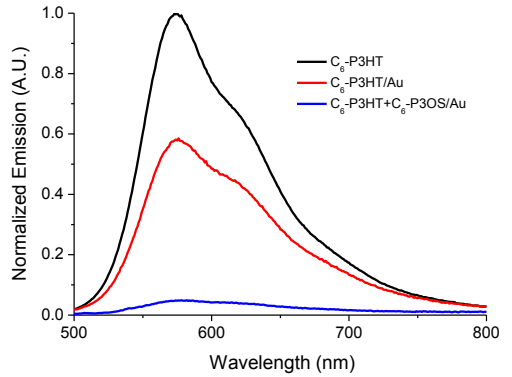

Figure 6. Normalized fluorescence spectra of **C6-P3HT**, **C6-P3HT/Au** and **C6-P3HT+C6-P3OS/Au**; spectra are corrected by the absorption of P3HT at 440 nm.

In order to be sure that the additional quenching originates from the vicinity between P3HT and P3OS on the Au surface, another hybrid is formed which is composed of P3OS anchored to Au as **C6-P3OS/Au**. Then **C6-P3HT/Au** and **C6-P3OS/Au** are mixed together in a 50/50 ratio and the fluorescence is measured. This allows us checking whether the quenching occurs simply because both P3HT and P3OS are together present in one sample, or whether it is necessary that the polymers are bound on the same NP. The UV-vis spectra of **C6-P3OS,** Au and **C6-P3OS/Au** are presented Figure 7 and show a red-shift of **C6-P3OS/Au** compared to **C6-P3OS** due to the anchoring of the CP onto the NP surface, as is also observed for **C6-P3HT/Au**.

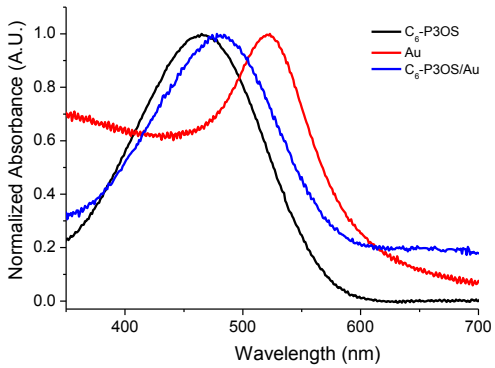

Figure 7. Normalized UV-vis spectra of, **C6-P3OS**, Au, **C6-P3OS/Au**; the spectra are measured in $CHCl_3$.

When measuring the emission spectra of **C6-P3HT/Au** and **C6-P3OS/Au**, it is clear that **C6-P3HT/Au** shows a much stronger emission upon excitation at 440 nm. When **C6-P3HT/Au** and **C6-P3OS/Au** are mixed in a 50/50 volume ratio, the emission signal also diminishes due to the

decreasing amount of **C_6-P3HT** present in the combined sample. However, the emission signal calculated by the averaged emission of **C_6-P3HT/Au** and **C_6-P3OS/Au**, also presented in the same graph, is in close agreement with the signal of the 50/50 mixture, indicating that there is no additional quenching as in the case of **C_6-P3HT+C_6-P3OS/Au**. This lets us conclude that the additional quenching originates from the anchoring of **C_6-P3HT** and **C_6-P3OS** on the same NP.

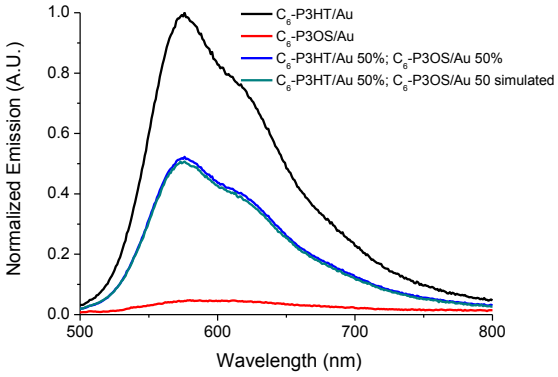

Figure 8. Normalized fluorescence spectra of **C_6-P3HT/Au**, **C_6-P3OS/Au** and the 50/50 mixture of **C_6-P3HT/Au** and **C_6-P3OS/Au**, together with the simulated 50/50 emission obtained from the original **C_6-P3HT/Au** and **C_6-P3OS/Au** samples.

CONCLUSION

In conclusion, air-stable protected thiol functionalized Ni-initiators, in which the linker between the aryl unit and the thiol functionality was varied, were prepared. These initiators allowed the controlled polymerization of P3HT and P3OS with control over the end-groups. Different CP/Au hybrids were formed by an *in situ* deprotection to the corresponding thiol. UV-vis and emission spectra were measured of the different hybrids, showing a stronger fluorescence quenching when the distance between the P3HT and the Au surface was decreased. Further fluorescence quenching could be realized by anchoring both P3HT and P3OS on the same NP.

ASSOCIATED CONTENT

Experimental procedures, ^{1}H NMR, ^{13}C NMR and ^{31}P NMR of all new compounds. ^{1}H NMR of the polymers and raw UV-vis and fluorescence spectra of the polymers and hybrids. This material is available free of charge via the Internet at http://pubs.acs.org.

AUTHOR INFORMATION

Corresponding Author

*E-mail: guy.koeckelberghs@chem.kuleuven.be

Funding Sources

Research Fund KU Leuven, the Fund for Scientific Research (FWO-Vlaanderen) and IWT doctoral fellowship for FM.

ACKNOWLEDGMENT

We are grateful to the Onderzoeksfonds KU Leuven/ Research Fund KU Leuven and the Fund for Scientific Research (FWO-Vlaanderen). FM and LV are grateful to IWT and FWO, respectively, for a doctoral fellowship and. WB thanks the KU Leuven for a postdoctoral mandate (PDM). The Mons laboratory is grateful to the 'Fonds National de la Recherche Scientifique' (FRS-FNRS) for financial support in the acquisition of the Waters QToF Premier mass spectrometer and for continuing support. We are grateful to Arne Billen for the TEM experiments.

REFERENCES

(1) Sheina, E. E.; Liu, J.; Iovu, M. C.; Laird, D. W.; Mccullough, R. D. *Macromolecules* **2004**, *37*, 3526–3528.

(2) Yokoyama, A.; Miyakoshi, R.; Yokozawa, T. *Macromolecules* **2004**, *37*, 1169–1171.

(3) Iovu, M. C.; Sheina, E. E.; Gil, R. R.; Mccullough, R. D. *Macromolecules* **2005**, *38*, 8649–8656.

(4) Miyakoshi, R.; Yokoyama, A.; Yokozawa, T. *Macromol. Rapid Commun.* **2004**, *25*, 1663–1666.

(5) Sui, A.; Shi, X.; Wu, S.; Tian, H.; Geng, Y.; Wang, F. *Macromolecules* **2012**, *45*, 5436–5443.

(6) Miyakoshi, R.; Shimono, K.; Yokoyama, A.; Yokozawa, T. *J. Am. Chem. Soc.* **2006**, *128*, 16012–16013.

(7) Yokoyama, A.; Kato, A.; Miyakoshi, R.; Yokozawa, T. *Macromolecules* **2008**, *41*, 7271–7273.

(8) Nanashima, Y.; Yokoyama, A.; Yokozawa, T. *Macromolecules* **2012**, *45*, 2609–2613.

(9) Stefan, M. C.; Javier, A. E.; Osaka, I.; McCullough, R. D. *Macromolecules* **2009**, *42*, 30–32.

(10) Huang, L.; Wu, S.; Qu, Y.; Geng, Y.; Wang, F. *Macromolecules* **2008**, *41*, 8944–8947.

(11) Wu, S.; Sun, Y.; Huang, L.; Wang, J.; Zhou, Y.; Geng, Y.; Wang, F. *Macromolecules* **2010**, *43*, 4438–4440.

(12) Bridges, C. R.; McCormick, T. M.; Gibson, G. L.; Hollinger, J.; Seferos, D. S. *J. Am. Chem. Soc.* **2013**, *135*, 13212–13219.

(13) Willot, P.; Govaerts, S.; Koeckelberghs, G. *Macromolecules* **2013**, *46*, 8888–8895.

(14) Pammer, F.; Passlack, U. *ACS Macro Lett.* **2014**, *3*, 170–174.

(15) Pammer, F.; Jäger, J.; Rudolf, B.; Sun, Y. *Macromolecules* **2014**, *47*, 5904–5912.

(16) Ono, R. J.; Kang, S.; Bielawski, C. W. *Macromolecules* **2012**, *45*, 2321–2326.

(17) Hollinger, J.; Jahnke, A. A.; Coombs, N.; Seferos, D. S. *J. Am. Chem. Soc.* **2010**, *132*, 8546–8547.

(18) Miyakoshi, R.; Yokoyama, A.; Yokozawa, T. *J. Am. Chem. Soc.* **2005**, *127*, 17542–17547.

(19) Jeffries-EL, M.; Sauvé, G.; McCullough, R. D. *Adv. Mater.* **2004**, *16*, 1017–1019.

(20) Jeffries-El, M.; Sauvé, G.; McCullough, R. D. *Macromolecules* **2005**, *38*, 10346–10352.

(21) Kochemba, W. M.; Pickel, D. L.; Sumpter, B. G.; Chen, J.; Kilbey, S. M. *Chem. Mater.* **2012**, *24*, 4459–4467.

(22) Kochemba, W. M.; Kilbey, S. M.; Pickel, D. L. *J. Polym. Sci. Part A Polym. Chem.* **2012**, *50*, 2762–2769.

(23) Pentzer, E. B.; Bokel, F. A.; Hayward, R. C.; Emrick, T. *Adv. Mater.* **2012**, *24*, 2254–2258.

(24) Okamoto, K.; Luscombe, C. K. *Chem. Commun.* **2014**, *50*, 5310–5312.

(25) Liu, J.; Mccullough, R. D. *Macromolecules* **2002**, *35*, 9882–9889.

(26) Lohwasser, R. H.; Thelakkat, M. *Macromolecules* **2010**, *43*, 7611–7616.

(27) Doubina, N.; Paniagua, S. a.; Soldatova, A. V.; Jen, A. K. Y.; Marder, S. R.; Luscombe, C. K. *Macromolecules* **2011**, *44*, 512–520.

(28) Monnaie, F.; Brullot, W.; Verbiest, T.; De Winter, J.; Gerbaux, P.; Smeets, A.; Koeckelberghs, G. *Macromolecules* **2013**, *46*, 8500–8508.

(29) Kaul, E.; Senkovskyy, V.; Tkachov, R.; Bocharova, V.; Komber, H.; Stamm, M.; Kiriy, A. *Macromolecules* **2010**, *43*, 77–81.

(30) Smeets, A.; Willot, P.; De Winter, J.; Gerbaux, P.; Verbiest, T.; Koeckelberghs, G. *Macromolecules* **2011**, *44*, 6017–6025.

(31) Smeets, A.; Van den Bergh, K.; De Winter, J.; Gerbaux, P.; Verbiest, T.; Koeckelberghs, G. *Macromolecules* **2009**, *42*, 7638–7641.

(32) Monnaie, F.; Ceunen, W.; De Winter, J.; Gerbaux, P.; Cocchi, V.; Salatelli, E.; Koeckelberghs, G. *Macromolecules* **2015**, *48*, 90–98.

(33) Van den Bergh, K.; Willot, P.; Cornelis, D.; Verbiest, T.; Koeckelberghs, G. *Macromolecules* **2011**, *44*, 728–735.

(34) Kempf, C. N.; Smith, K. a.; Pesek, S. L.; Li, X.; Verduzco, R. *Polym. Chem.* **2013**, *4*, 2158.

(35) Xu, J.; Wang, J.; Mitchell, M.; Mukherjee, P.; Jeffries-EL, M.; Petrich, J. W.; Lin, Z. *J. Am. Chem. Soc.* **2007**, *129*, 12828–12833.

(36) Liu, J.; Tanaka, T.; Sivula, K.; Alivisatos, a P.; Fréchet, J. M. J. *J. Am. Chem. Soc.* **2004**, *126*, 6550–6551.

(37) Li, Z.; Berger, H.; Okamoto, K.; Zhang, Q.; Luscombe, C. K.; Cao, G.; Schlaf, R. *J. Phys. Chem. C* **2013**, *117*, 13961–13970.

(38) Senkovskyy, V.; Khanduyeva, N.; Komber, H.; Oertel, U.; Stamm, M.; Kuckling, D.; Kiriy, A. *J. Am. Chem. Soc.* **2007**, *129*, 6626–6632.

(39) Senkovskyy, V.; Tkachov, R.; Beryozkina, T.; Komber, H.; Oertel, U.; Horecha, M.; Bocharova, V.; Stamm, M.; Gevorgyan, S. A.; Krebs, F. C.; Kiriy, A. *J. Am. Chem. Soc.* **2009**, *131*, 16445–16453.

(40) Sontag, S. K.; Marshall, N.; Locklin, J. *Chem. Commun. (Camb).* **2009**, 3354–3356.

(41) Marshall, N.; Sontag, S. K.; Locklin, J. *Macromolecules* **2010**, *43*, 2137–2144.

(42) Tkachov, R.; Senkovskyy, V.; Horecha, M.; Oertel, U.; Stamm, M.; Kiriy, A. *Chem. Commun. (Camb).* **2010**, *46*, 1425–1427.

(43) Winter, J. De; Deshayes, G.; Boon, F.; Coulembier, O.; Dubois, P.; Gerbaux, P. *J. Mass Spectrom.* **2011**, *46*, 237–246.

(44) Verswyvel, M.; Steverlynck, J.; Hadj Mohamed, S.; Trabelsi, M.; Champagne, B.; Koeckelberghs, G. *Macromolecules* **2014**, *47*, 4668–4675.

(45) Keating, C. D.; Musick, M. D.; Keefe, M. H.; Natan, M. J. *J. Chem. Educ.* **1999**, *76*, 949–955.

(46) Liu, J.; Loewe, R. S.; McCullough, R. D. *Macromolecules* **1999**, *32*, 5777–5785.

(47) Brust, M.; Walker, M.; Bethell, D.; Schiffrin, D. J.; Whyman, R. *J. Chem. Soc., Chem. Commun.* **1994**, 801–802.

(48) Saha, K.; Agasti, S. S.; Kim, C.; Li, X.; Rotello, V. M. *Chem. Rev.* **2012**, *112*, 2739–2779.

(49) Dulkeith, E.; Morteani, A. C.; Niedereichholz, T.; Klar, T. A.; Feldmann, J.; Levi, S. A.; van Veggel, F. C. J. M.; Reinhoudt, D. N.; Möller, M.; Gittins, D. I. *Phys. Rev. Lett.* **2002**, *89*, 203002.

(50) Ma, N.; Tang, F.; Wang, X.; He, F.; Li, L. *Macromol. Rapid Commun.* **2011**, *32*, 587–592.

Table of Contents Graphic and Synopsis

Influence of Structure of End-group Functionalized Poly(3-hexylthiophene) and Poly(3-octylselenophene) Anchored on Au Nanoparticles

Frederic Monnaie, Lize Verheyen, Julien De Winter, Pascal Gerbaux, Ward Brullot, Thierry Verbiest, and Guy Koeckelberghs